Atomistic simulations of formation and stability of carbon nanorings

P. Liu,[1] Y. W. Zhang,[2,*] and C. Lu[1]
[1]*Institute of High Performance Computing, Singapore 117528*
[2]*Department of Materials Science and Engineering, National University of Singapore, Singapore 119260*
(Received 21 February 2005; revised manuscript received 15 June 2005; published 7 September 2005)

Atomistic simulations of the formation and stability of nanorings through the energy relaxation of geometrically folded single-walled carbon closed rings are performed using the second-generation reactive bond-order potential. It is found that the critical diameter for forming a stable nanoring can be made significantly smaller than that observed in experiments. The critical diameter for an armchair nanoring is smaller than that for a zigzag nanoring with the same nanotube diameter. The effect of torsion on a nanoring reduces its critical diameter. A large flattening of the nanotube cross section is found to be effective for the reduction in stress and stiffness of the nanoring. In addition, the instability of a nanoring always starts with the formation of short wavelength ripples on the compressed side of the nanotube. Subsequently, some ripples will develop into buckles, resulting in buckling failures.

DOI: 10.1103/PhysRevB.72.115408 PACS number(s): 61.46.+w, 73.22.−f, 62.25.+g, 64.70.Nd

I. INTRODUCTION

Carbon nanotubes are ideal candidates for the basic building blocks of nanoelectronic and nanomechanical devices due to their fascinating mechanical and electronic properties.[1] Recently, nanorings, which are a variant of nanotubes, have attracted great research interest. These nanorings are of unusual properties which are interesting for both the fundamental understanding and the development of nanodevices. For example, the negative magnetoresistance and weak electron-electron interactions of the nanoring in the low temperature regime were observed.[2] Depending on the circumstance length of the ring, a transition from *n*-type semiconducting to conducting behavior was observed experimentally and the rectification properties of a carbon nanotube ring transistor were demonstrated.[3] In addition, the persistent currents in the ring yielded valuable information to understand both quantum coherence and dephasing rates.[4] So far several experimental occurrences of nanoring structures have been reported.[5–10] Currently the synthesized carbon rings have a relatively large diameter, within the range of 200–700 nm.[5–10]

The formation and structures of carbon nanorings have been subjected to extensive theoretic and modeling analysis.[11–18] For example, the energetics and structures of nanotube rings were analyzed by tight-binding and semi empirical quantum mechanical approaches,[11] classic molecular dynamics approaches,[12–16] continuum mechanics approaches,[17] and thermodynamics approaches.[18] It is understood through these analyses that a carbon nanoring can be made of either pure hexagons or a mixture of hexagons and topological pentagon-heptagon defects. It is believed that the nanorings with a pure hexagon structure is more energetically favorable when the nanoring diameter is large, while the nanoring with a mixture of hexagons and pentagon-heptagon defects is more energetically favorable when the nanoring diameter is small.[14,17] For the former, the bending deformation accommodates the ring curvature, while for the latter, the pentagon-heptagon defects are incorporated to accommodate the ring curvature.

To improve electronic performance of nanodevices, it is highly desirable to reduce the diameter and the number of defects (pentagons and heptagons) of carbon nanotube rings. One way to achieve this is to geometrically bend a defect-free single-walled straight nanotube into a circular ring by connecting its two ends so that no defects such as pentagons or heptagons are introduced.[12–16] The formation of such stable nanotube rings involves the formation of covalent bonds by joining two nanotube ends. Before the formation of the bonds, the nanotube must be bent to allow its two ends to join. Thus the strain energy arising from bending a straight nanotube into a closed ring forms an energy barrier. It is known that the smaller the ring diameter, the higher the strain energy per atom and thus the higher the energy barrier.[17] Hence external work must be done to overcome the closed-ring formation barrier.

Theoretic and modeling analyses on bending of a straight nanotube into a nanoring have been performed.[11–18] It is understood that for a fixed nanotube diameter and helicity, there is a critical nanotube length (or a critical ring diameter), above which the ring is stable while below which unstable bending deformation occurs, resulting in rippling and buckling of the ring.[12–16] It is also found that nanotubes with smaller diameters will form perfect nanoring structures of smaller ring diameters and the cross-section deforms elliptically.[12–16] In addition, it has been shown that the buckling of a nanotube under uniform bending conditions may result in the transition from a delocalized to a localized deformation and lead to a dramatic reduction in the electric conductance.[15] The applicability of elastic shell theory to the bending of nanotubes is still debatable. On the one hand, elastic shell theory has been frequently used to analyze the bending deformation of nanotubes.[17–19] On the other hand, molecular dynamics simulations have shown that elastic shell theory fails to describe the formation of multiple buckles.[15]

In the present work, atomistic simulations using the second-generation reactive bond-order potential were performed to systematically investigate the formation and stability of carbon nanorings. Our interest here is to focus on

the stability of bending a carbon nanotube into a defect-free nanoring, with an emphasis on the influences of the helicity and torsion of the nanotubes and the applicability of elastic shell theory.

II. MODEL

To simulate the formation and stability of a nanoring, a single-walled straight armchair or zigzag nanotube is first geometrically bent into a circular ring by connecting its two ends. The advantages of this operation are that there is no ambiguity in the boundary condition and no defects such as pentagons or heptagons are introduced. The geometrically bent nanoring is then subjected to energy relaxation. The stability of the nanorings should depend on the system parameters, such as the diameter, length, helicity, and torsion of the nanotube. The interactions of carbon atoms in the nanoring are governed by the second-generation reactive empirical bond-order potential.[20] This potential uses improved analytical functions and an extended database, leading to a much improved description of chemical and mechanical properties for hydrogen molecules, diamond, and nanotubes.[20,21] In the present atomistic simulations, the Verlet integration scheme is used with a time step size of 1.05×10^{-15} s. The relaxation uses a method similar to a gradient cooling method[12] by selectively damping atomic velocities. If the dot product of the velocity vector and acceleration vector for an atom is positive, no damping is applied to the atom. Otherwise, a damping factor of 0.95 is applied to the velocity of the atom.

III. RESULTS AND DISCUSSIONS

Four armchair configurations: (3,3), (4,4), (5,5), and (6,6) and four zigzag configurations: (5,0), (7,0), (9,0), and (10,0) of carbon nanotubes are used in the present study. The nanotube diameters d for the four armchair configurations are 0.407, 0.542, 0.678, and 0.814 nm, respectively, and the nanotube diameters d for the four zigzag configurations are 0.391, 0.548, 0.705, and 0.783 nm, respectively. For a straight nanotube with a length of L, the diameter of its geometrically folded ring is $D=L/\pi$. To estimate the critical diameter D_c for a stable nanoring, various initial diameters D of the folded nanorings ranging from 1.96 to 19.65 nm were used. Torsion was also included to analyze the stability of nanorings. The torsion nanorings were obtained by axially rotating the cross section of one end of a straight nanotube by 360° relatively to the other end, followed by geometrically bending the rotated tube into a circular ring with its two ends connected. The nanotube configurations and the nanoring diameters mentioned above were also used to study the torsion effect.

During the energy relaxations, the potential energy change per atom for a stable ring is smaller than that of an unstable ring for the same tube type. For example, the amount of energy reduction between the initial and final relaxed configurations is 0.40 eV per atom for the stable (5,5) ring with an initial ring diameter of 11.79 nm; while it is 0.98 eV per atom between the initial and final relaxed configurations for an unstable (5,5) ring with an initial ring diameter of 7.86 nm. Thus the potential energy per atom suffers a larger drop for a buckled ring. Figure 1 shows the variations of the approximate critical diameter of a stable nanoring D_c with its nanotube diameter d for the following three situations: armchair configuration without torsion, armchair configuration with torsion, and zigzag configuration with torsion. Figure 1 allows several observations to be made. First, the critical diameters for stable nanorings can be as low as a few nanometers which are significantly smaller than 200–700 nm observed in experiments.[5–10] The reason for this difference is due to the energy barrier for ring formation. To overcome the energy barrier, far-from equilibrium processing conditions are required. However, these experiments were performed at near-equilibrium conditions, and thus could only lead to the nanorings with large diameters.[5–10] Second, the critical diameter D_c of the nanoring increases with an increase in nanotube diameter d, which is consistent with the simulation and analysis results in Refs. 11–18. This observation, which is applicable to both armchair and zigzag types and to the configurations with and without torsion, can be qualitatively explained by elastic shell theory: for the same value of ring diameter D, the larger the nanotube diameter d, the higher the atomic stress, thus the strain energy per atom is higher. The ring loses its stability when the increase in strain energy exceeds the reduction in the end-connection bonding energy. However, quantitatively there is a discrepancy between the D_c versus d relationship predicted by elastic shell theory and that predicted by the present atomistic simulations. The elastic shell theory predicts that D_c increases slowly and superlinearly with d.[22] But the present study shows a nearly linear relationship with a large slope when d is larger than 0.55 nm. The reason for this discrepancy is likely due to the difference between the change of tube cross-section shape predicted by elastic shell theory[23,24] and that predicted by the present atomistic simulations. This point will be discussed in more detail shortly. Third, the critical diameter of a nanoring with torsion is smaller than that without torsion for the same nanotube diameter, indicating that torsion has a positive effect on the stability of the nanorings. For example, the critical diameters of the (4,4) configuration with and without

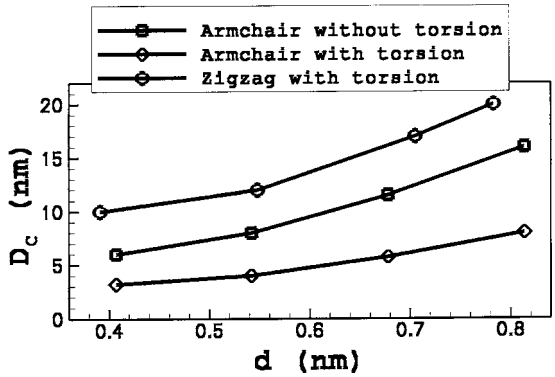

FIG. 1. Critical nanoring diameter D_c vs nanotube diameter d for armchair configurations without torsion, armchair configurations with torsion and zigzag configurations with torsion. For the same nanotube diameter, the addition of torsion is of a positive effect for nanoring stability and the critical diameter with the armchair type is smaller than that with the zigzag type.

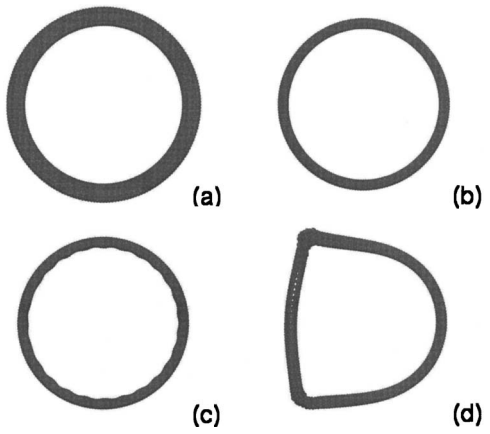

FIG. 2. The deformation sequence of an armchair (5,5) nanoring with an initial diameter $D=7.86$ nm without torsion during relaxation. (a) Before relaxation, (b) the shrinkage of nanoring diameter and the flattening of the cross section, (c) the appearance of ripples, and (d) the development of buckles.

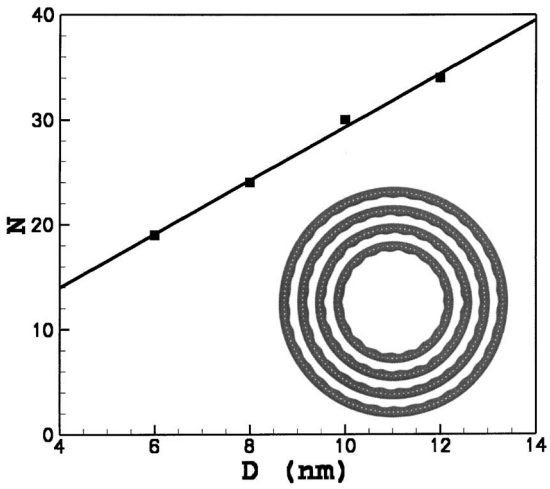

FIG. 3. Number of ripples N vs the nanoring diameter D of the (6,6) type without torsion. The diameters of the nanorings in the inset are 5.89, 7.86, 9.82, and 11.79 nm, respectively. A linear relationship is observed between the number of ripples N and the nanoring diameter D.

torsion are approximately 3.93 and 7.86 nm, respectively. This phenomenon, which is also observed for the zigzag configurations, is in contrast to the elastic shell model, which predicts that the inclusion of torsion further increases the nanoring strain energy and results in a larger stable ring diameter.[23] The failure of the elastic model may owe to the unique deformation pattern of the torsion rings, which will be discussed later in detail. Finally, the critical diameter for an armchair configuration is smaller than that for a zigzag configuration with the same nanotube diameter, indicating under bending deformation, the armchair configuration is more stable than the zigzag configuration. This phenomenon has also been observed in Ref. 12. This difference may be due to the difference in bonding conditions in the armchair and zigzag configurations. In zigzag nanotubes, one-third of the bonds are aligned along the axial direction of the tubes, however, for armchair nanotubes, one-third of the bonds are perpendicular to the axial direction of the tubes.

It is found that there is a series of events occurring during the relaxation of a ring without torsion. The diameter of the nanoring shrinks gradually during the relaxation. If such a ring is stable, the diameter of the nanoring shrinks and finally reaches a constant, and the deformation along the circumferential direction is homogeneous. If such a ring is unstable, ripples develop at the compressive side of the nanoring, followed by the formation of buckles, which causes the formation of an irregular polygon structure. Figures 2(a)–2(d) show a typical unstable deformation sequence during the energy relaxation of an armchair (5,5) nanoring with an initial diameter of $D=7.86$ nm without torsion. It is found that when comparing the initial configuration as shown in Fig. 2(a) and the relaxed configuration shown in Fig. 2(b), the diameter of the nanoring shrinks markedly, while, the cross-section of the nanoring flattens significantly. Subsequently, ripples develop at the compressive side of the nanoring as shown in Fig. 2(c). Soon after, buckles develop as shown in Fig. 2(d). For unstable nanorings from a nanotube of the same diameter, it is found that the number of ripples N increases with an increase in the diameter D of the nanoring approximate linearly. This can be seen from Fig. 3 and its inset. This linear relation is in contrast to the prediction by elastic shell theory that the number of ripples N is proportional to the square root of the nanoring diameter D.[16] The present results show that only a small number of the ripples develop into buckles, while the majority of the ripples disappear.

Similar to a nanoring without torsion, the diameter of the nanoring with torsion also shrinks gradually during the energy relaxation. If such a ring with torsion is stable, the diameter of the nanoring shrinks and finally reaches a constant. However, the deformation along the circumferential direction is not homogeneous during the energy relaxation. The stable ring adopts a regular polygonal shape with uniformly distributed apexes formed along the circumference. This can be clearly seen from Fig. 4 which shows a stable (6,6) ring with a ring diameter of $D=7.86$ nm. For an unstable torsion ring, some of apexes develop into buckles, while other apexes disappear, and subsequently the ring loses its stability. Figures 5(a)–5(d) show this deformation sequence of an unstable zigzag (7,0) nanoring with an initial diameter of $D=7.86$ nm with torsion.

It is noted that the spacing of apexes of a ring with torsion is much larger than the spacing of ripples of the same ring without torsion. This is evident by comparing Fig. 4 with Fig. 6 which shows the ripple distribution for the unstable (6,6) ring with a ring diameter of $D=7.86$ nm without torsion. This increase in apex spacing may be used to explain why torsion plays a stabilizing effect on the ring formation. For the stable torsion ring adopting a polygonal shape as shown in Fig. 4, large curvature changes are concentrated at the apexes to accommodate most of the bending deformation, while the sides of the polygon remain nearly straight and thus deform only slightly. It is noted that both the present results (for example, Fig. 5) and that in Ref. 16 show that for an unstable ring, further energy minimization results in a subsequent reduction of the number of apexes, making bend-

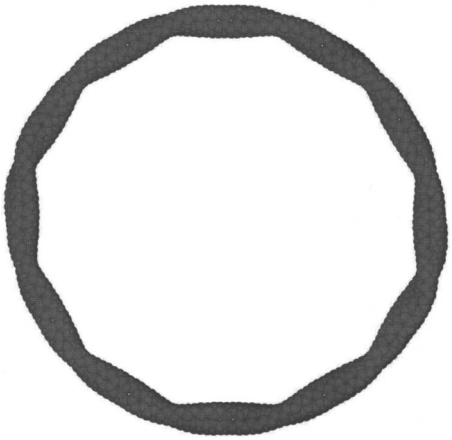

FIG. 4. Final stable configuration of the (6,6) ring with a ring diameter of 7.86 nm with torsion. The stable ring adopts a regular polygonal shape. Large curvature changes are concentrated at the apexes to accommodate most of the bending deformation, while the sides of the polygon remain nearly straight and thus deform only slightly.

ing deformation more and more concentrated at these left apexes, therefore resulting in an overall reduction of total energy. Since the addition of torsion causes the formation of apexes, making bending deformation also concentrated at these apexes, this should also result in a reduction of total energy and therefore give rise to the stabilizing effect.

During energy relaxation, the cross section of the nanoring flattens significantly as shown in Fig. 7. Both the compressive and tensile parts of the nanotube wall form nearly flat planes, which are parallel to each other. It is observed from Fig. 7 that the distance between the planes is approximately a constant and nearly independent of the diameter of the nanotube. As expected, the distance is approximately 0.34 nm, which is the interlayer spacing of graphite.

Elastic shell theory has been widely used to predict the deformation and bifurcation of macroscopic cylindrical tubes

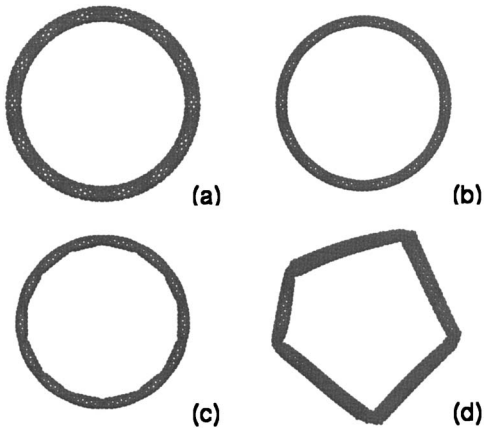

FIG. 5. Deformation sequence of a zigzag (7,0) nanoring with an initial diameter $D=7.86$ nm with torsion during relaxation. (a) Before relaxation, (b) the shrinkage of nanoring diameter and the flattening of the nanotube cross section, (c) the appearance of apexes, and (d) the development of buckles. The apex spacing with torsion is larger than the ripple spacing without torsion.

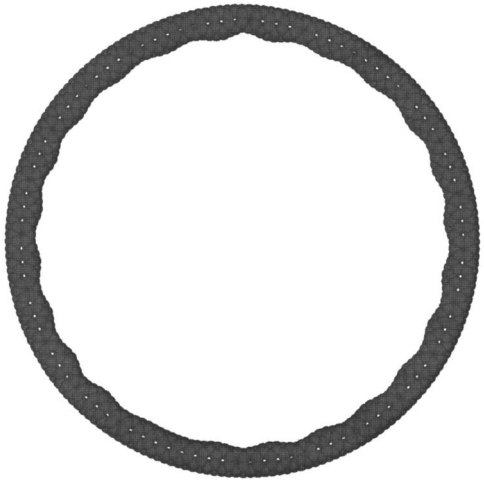

FIG. 6. Unstable configuration at ripple formation for the same initial ring as Fig. 4 but without torsion. The spacing of apexes in Fig. 4 is much larger than the spacing of ripples without torsion shown here.

under bending.[22–25] For a relatively thin-walled macroscopic tube, the theory predicts that its bending will lead to an "ovalization" (an elliptical shape) at the tube cross section. The growth of ovalization causes a progressive reduction in the bending rigidity of the wall. Short wavelength ripples were observed on the compressed side of the shell when the curvature and ovalization reach a certain critical level. Finally, a maximum value of the moment is reached and further bending will cause a drop in the bending moment due to buckling. The critical shape of the elastic tube cross section is shown Fig. 8.[24] Apparently elastic macroscopic tubes and carbon nanotubes share some similarities in their buckling processes, thus elastic shell theory is able to predict the bending deformation of carbon nanorings qualitatively. However, comparing Figs. 7 and 8, one may find that the cross section shape of the tubes predicted by elastic shell theory is

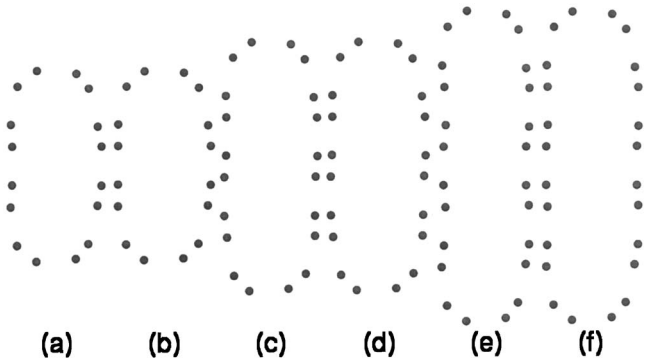

FIG. 7. Flattened cross sections for different nanotube configurations and nanoring diameters D. (a) (4,4) and $D=7.86$ nm, (b) (4,4) and $D=15.72$ nm, (c) (5,5) and $D=11.79$ nm, (d) (5,5) and $D=15.72$ nm, (e) (6,6) and $D=7.86$ nm, and (f) (6,6) and $D=11.79$ nm. The cross sections for (a), (b), (c), and (d) are the final stable configurations while the cross sections for (e) and (f) are the configurations just prior to the ripple formation. It can be seen that the distance between the two flattening nanotube walls is approximately constant and is in fact 0.34 nm.

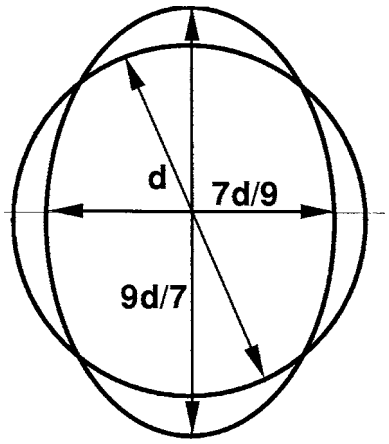

FIG. 8. Critical cross-sectional shape of an elastic tube under bending for instability predicted by elastic shell theory. The dotted circle stands for the initial shape of an elastic tube cross section with diameter d. The solid ellipse stands for the critical cross section for bending instability; the major axis is $9d/7$ and the minor axis is $7d/9$ Ref. 24.

different from that predicted by the present atomistic simulations. Hence elastic shell theory does not quantitatively predict the change of cross section of nanorings. Obviously the flattened cross section is an effective way to reduce the bending stiffness and stress, and the larger the nanotube diameter, the more effective the bending stiffness reduction. In addition, the flattening of the cross sections with an approximate wall-wall distance of the graphitic interlayer spacing may explain the nearly linear relationship between the critical ring diameter and the nanotube diameter when the nanotube diameter is larger than 0.55 nm.

Previous studies showed that the defect-free ring configuration in which strain is uniformly distributed is more stable for rings with large diameters, while the ring with localized pentagon-heptagon defects is more stable for rings with small diameters.[14,17] The ring diameters used in the present study fall into the small diameter category. However, our simulation results show that although hexagonal bonding configuration is deformed, no pentagon-heptagon defects are formed. This may be explained by the energy barrier for forming the pentagon-heptagon defects.[12] In the present simulations, the rings are initially defect-free. To form such defects, large thermal activation energy is required.[12] But there is negligible thermal activation energy during the present ring relaxation process. Thus no pentagon-heptagon defects are formed.

Although several atomistic simulations have been performed to study the deformation and stability of nanoring through bending straight nanotubes,[10–16] it is noted that some reported results are not consistent. For example, the critical diameter for the formation of a stable nanoring through bending a (5,5) armchair nanotube is 3.9 nm obtained using the order-N nonorthogonal tight-binding molecular dynamics,[15] 6.0 nm obtained using the first generation reactive bond-order potential,[14] and 14.3 nm obtained also using the first generation reactive bond-order potential.[16] The present result using the second generation reactive bond-order potential is approximately 11.79 nm. It appears that different atomistic potentials and relaxation schemes may affect the simulation results. Thus more accurate approaches are required to eliminate these uncertainties.

IV. CONCLUSIONS

The stability of a single-walled carbon nanotube-based nanoring has been investigated using atomistic simulations with the second generation empirical bond-order potential. It is found that the critical diameter for a stable nanoring depends on system parameters, such as the diameter, length, helicity, and torsion of the nanotube. The unstable deformation sequence of nanorings and macroscopic tubes share some similarities. It is found that elastic shell theory is able to predict the deformation and failure of nanorings qualitatively. However, its explanation of the effects of the helicity, torsion, and large flattening of the cross section is not satisfactory.

*Author to whom correspondence should be addressed. Electronic address: msezyw@nus.edu.sg

[1] R. H. Baughman, A. A. Zakhidov, and W. A. de Heer, Science **297**, 787 (2002).
[2] H. R. Shea, R. Martel, and P. Avouris, Phys. Rev. Lett. **84**, 4441 (2000).
[3] H. Watanabe, C. Manabe, T. Shigematsu, and M. Shimizu, Appl. Phys. Lett. **78**, 2928 (2001).
[4] S. Latil, S. Roche, and A. Rubio, Phys. Rev. B **67**, 165420 (2003).
[5] J. Liu, H. J. Dai, J. H. Hafner, D. T. Colbert, R. E. Smalley, S. J. Tans, and C. Dekker, Nature (London) **385**, 780 (1997).
[6] R. Martel, H. R. Shea, and P. Avouris, Nature (London) **398**, 299 (1999).
[7] R. Martel, H. R. Shea, and P. Avouris, J. Phys. Chem. B **103**, 7551 (1999).
[8] M. Ahlskog, E. Seynaeve, R. J. M. Vullers, C. Van Haesendonck, A. Fonseca, K. Hernadi, and J. B. Nagy, Chem. Phys. Lett. **300**, 202 (1999).
[9] E. Flahaut, A. Peigney, C. Laurent, and A. Rousset, J. Mater. Chem. **10**, 249 (2000).
[10] M. Sano, A. Kamino, J. Okamura, and S. Shinkai, Science **293**, 1299 (2001).
[11] D. H. Oh, J. M. Park, and K. S. Kim, Phys. Rev. B **62**, 1600 (2000).
[12] M. Huhtala, A. Kuronen, and K. Kaski, Comput. Phys. Commun. **146**, 30 (2002).
[13] M. Huhtala, A. Kuronen, and K. Kaski, Comput. Phys. Commun. **147**, 91 (2002).
[14] J. Han, Chem. Phys. Lett. **282**, 187 (1998).
[15] L. Liu, C. S. Jayanthi, and S. Y. Wu, Phys. Rev. B **64**, 033412 (2001).

[16] O. Hod, E. Rabani, and R. Baer, Phys. Rev. B **67**, 195408 (2003).
[17] V. Meunier, Ph. Lamin, and A. A. Lucas, Phys. Rev. B **57**, 14886 (1998).
[18] S. Zhang, S. Zhao, M. Xia, E. Zhang, and T. Xu, Phys. Rev. B **68**, 245419 (2003).
[19] B. I. Yakobson, C. J. Brabec, and J. Bernholc, Phys. Rev. Lett. **76**, 2511 (1996).
[20] D. W. Brenner, O. A. Shenderova, J. A. Harrison, S. J. Stuart, B. Ni, and S. B. Sinnott, J. Phys.: Condens. Matter **14**, 783 (2002).
[21] O. A. Shenderova, D. W. Brenner, A. Omeltchenko, X. Su, and L. H. Yang, Phys. Rev. B **61**, 3877 (2000).
[22] X. Wang and J. Cao, J. Eng. Mater. Technol. **123**, 430 (2001).
[23] S. Timoshenko and J. M. Gere, *Theory of Elastic Instability*, (McGraw-Hill, New York, 1961).
[24] L. G. Brazier, Proc. R. Soc. London, Ser. A **116**, 104 (1927).
[25] S. Kyriakides and G. T. Ju, Int. J. Solids Struct. **29**, 1117 (1992).